Osteoarthritis and Cartilage (2001) **9,** 463–472
© 2001 OsteoArthritis Research Society International
doi:10.1053/joca.2001.0413, available online at http://www.idealibrary.com on IDEAL®
1063–4584/01/050463+10 $35.00/0

Osteoarthritis and Cartilage
Journal of the OsteoArthritis Research Society International

High-resolution MRI detects cartilage swelling at the early stages of experimental osteoarthritis

E. Calvo*, I. Palacios*, E. Delgado†, J. Ruiz-Cabello‡, P. Hernández*, O. Sánchez-Pernaute*, J. Egido* and G. Herrero-Beaumont*

**Department of Orthopaedic Surgery, Rheumatology Service and Inflammation Research Unit, Fundación Jiménez Díaz, Universidad Autónoma, Madrid, Spain; †Department of Morphology, Hospital La Paz, Universidad Autónoma, Madrid, Spain; ‡Magnetic Resonance Imaging Research Laboratory, Instituto Pluridisciplinar, Universidad Complutense, Madrid, Spain*

Summary

Objective: The progressive early changes in cartilage and subchondral bone in an experimental model of osteoarthritis (OA) were investigated with high-resolution magnetic resonance imaging (MRI) and microradiography.

Methods: Partial medial meniscectomy was performed in the left knee of 16 rabbits. Four normal and four sham-operated additional rabbits were used as controls. Changes in cartilage and subchondral bone were sequentially assessed after surgery with MRI at 0, 2, 4, 6, 8 and 10 weeks, subchondral bone variations quantified postoperatively on microradiographs of sagittal sections at 6 and 10 weeks and the macroscopic alterations graded according to the severity of joint changes.

Results: MRI demonstrated a progressive increase in the articular cartilage thickness in the weight-bearing area of the femur at weeks 4, 6 and 8 vs basal. Tibial cartilage thickness only showed a significant increment at week 6. No significant abnormalities were detected on X-rays in subchondral bone when compared to controls. Macroscopically, 4 weeks after the operation OA rabbits had only slight cartilage discoloration. Cartilage eburnation, pitting, superficial erosions and osteophytes were detected at week 6. These abnormalities were more evident at 8 and 10 weeks after meniscectomy.

Conclusion: The focal increase in cartilage thickness is one of the earliest measurable changes in OA and preceeds subchondral bone remodeling. The measurement of cartilage thickness variations with MRI can be used to follow the course of OA and to evaluate the potential beneficial effect of novel therapies.

Key words: Magnetic resonance imaging, Osteoarthritis, Cartilage, Subchondral bone.

Introduction

Osteoarthritis (OA) is a heterogeneous group of conditions associated with defective integrity of articular cartilage, subchondral bone and synovium[1]. However, it is not yet clearly understood which of them is first or predominantly affected at the early stages of the disease[2]. These limitations in the knowledge of OA are partly due to the absence of valuable means to detect early changes or to follow the natural history of the disease in individual patients. Because of the lack of specific early signs, OA can only be recognized with certainty relatively late in its course. However, a firm early diagnosis is desirable because the sooner treatment is instituted the more effective is likely to be. The diagnosis of OA and the evaluation of its progression still rely mainly on conventional radiography. Radiography permits only indirect evaluation of articular cartilage degeneration based on joint space narrowing and is incapable of demonstrating early lesions in the internal structure of cartilage. More specific radiographic signs, such as bone sclerosis, cysts or osteophytes occur later in the disease and progress slowly. Thus, radiography is of very limited value in early detection of OA and assessment of its short-term progression. Other diagnostic methods, such as arthrography, arthroscopy, computed tomography or ultrasounds have clear disadvantages, such as their invasiveness and limited visualization of cartilage, and they are not sensitive enough for assessing short-term OA evolution[3].

Magnetic resonance imaging (MRI), by virtue of its superior soft tissue contrast, high spatial resolution, multiplanar capability, and ability to allow direct visualization of the cartilage, appears to be ideally suited for the investigation of joint diseases. Because it is non-destructive, several parameters can be evaluated in the same specimen[3–5]. Moreover, the technique is non-invasive and sufficiently well tolerated by patients to justify frequent serial examinations of even asymptomatic joints. Despite its theoretical advantages, acceptance of MRI for this particular indication has been slow, mainly because the earlier MR techniques lacked sufficient spatial resolution and provided poor contrast between the cartilage and

Received 18 April 2000, revision requested 10 July 2000, revision received 20 September 2000; accepted 10 January 2001.
Supported by a grant from: Boehringer Ingelheim.
Address correspondence to: Gabriel Herrero-Beaumont, MD, Inflammation Research Unit, Rheumatology Service, Fundación Jiménez Díaz, UAM, Avda. Reyes Católicos, 2, 28040 Madrid, Spain. Tel: 34-91-550 4800; Fax: 34-91-549 4764; E-mail: Gherrero@fjd.es

adjacent structures[6]. However, continuous improvements in coil design and gradient performance along with the development of more efficient pulse sequences and new methods of enhancing contrast among articular structures have overcome many of these problems[4,7–10].

Numerous studies have evaluated the articular cartilage in OA with MRI. Many of them have compared the ability of MRI to other diagnostic methods—planar radiography[11–13], computed tomography[14], arthroscopy[11,12], and pathology[10,12,15]—to detect focal cartilaginous abnormalities. Others used MRI to differentiate in hyaline cartilage lamina of different intensity which have been correlated with those seen histologically[16,17] and have assessed the alterations in intensity and distribution of these lamina in OA[10,18,19]. A few authors have also analyzed the changes in the MRI appearance of subchondral bone in this disease[19,20–22]. Although recent attention has been focused on the quantification of hyaline cartilage distribution under normal and pathologic conditions[8,23–25], the reports of longitudinal studies monitoring the quantitative changes in subchondral bone and cartilage in the early stages of the disease are scant[21,26]. The objectives of the present study were (1) to measure the progressive early variations in cartilage and subchondral bone sclerosis based on a 4.7 T system equipped with a microimaging gradient coil and (2) to quantify early subchondral bone changes using microscopic radiography in a partial meniscectomy experimental model of OA in the rabbit knee[27].

Materials and methods

EXPERIMENTAL ANIMAL MODEL

A total of 24 white New Zealand male rabbits (8 weeks old, 2.0–2.5 kg) were obtained from B&K Universal, Madrid, Spain. Group I, 16 rabbits, underwent left partial medial meniscectomy to experimentally induce degenerative knee lesions. Ten of these rabbits were used for longitudinal MRI preoperatively and 2, 4, 6, 8 and 10 weeks after the operation to characterize the progression of their stifle joint disease. Meniscectomized rabbits were euthanized by intracardiac administration of sodium pentobarbital (50 mg/kg) (Pentotal, Abbott, Madrid, Spain) at 2 weeks (two animals), 4 weeks (two animals), 6 weeks (five animals), 8 weeks (two animals), and 10 weeks (five animals). The operated knees were evaluated for gross pathologic abnormalities and these changes were correlated with MRI findings in the animals imaged. Histoquantitation of subchondral bone was performed in the rabbits euthanized at 6 and 10 weeks. Group II (four rabbits) represented a sham-operated series, and group III (four rabbits) a further control series comprising normal left knees. Two animals of each control group were euthanized at 6 and 10 weeks respectively and their knees examined for macroscopic and radiographic changes. The research complied with national legislation and with the National Institute of Health Guide for the Care and Use of Laboratory Animals.

Rabbits were anesthetized by intramuscular injection 2 ml/kg of xylazine (Rompun, Bayer Leverkusen, Madrid, Spain) and ketamine HCl (Ketolar, Parke-Davis, Barcelona, Spain) 5:1, and a partial medial meniscectomy was performed in the left knee. Antibiotic prophylaxis was administered with cefonicid (100 mg/kg) (Monocid, Smith and Beecham, Madrid, Spain). Under sterile conditions, the knee was approached via median parapatellar incision. Using iris scissors, the meniscotibial ligament was incised, the peripheral attachment of the anterior one-half of the meniscus was released and finally excised. The knee was closed by layers and a bulky Robert-Jones bandage applied with the knee bent at 90° for four days. All animals were permitted free cage activity after surgery. The sham-operated rabbits underwent the same procedure with the exception of meniscectomy.

MRI

Animals were anesthetized following the same protocol and MRI of the left knee was performed on a Bruker Biospec 47/40 spectrometer (Bruker Medizintechnik GmBH, Ettlingen, Germany) equipped with a 4.7 T superconducting magnet (Oxford Instruments Ltd, Oxford, U.K.) and high-performance unshielded gradients with a maximum gradient strength of 300 mT/m. The rabbit was laid in the supine position on a Plexiglas support bed with the operated knee extended and introduced into the magnet. The radiofrequency probe used was a customized circular birdcage type resonator operating in the single-coil transmit/receive mode. The support bed was a semi-cylinder with a diameter equal to the inner surface of the magnet and its surface had a specially located adhesive tapes where the coil was reproducibly attached. This coil was a low-pass (eight columns) design consisting of two plastic cylinders: the outer cylinder acted as a shield to diminish receiver losses, improve the signal to noise ratio and decrease radiation losses that increased with the resonance frequency, while the inner cylinder functioned as a knee holder that immobilized completely the joint in full extension and placed it precisely in the isocenter of the magnet.

The imaging acquisition protocol started with two sets of pilot scans using a fast spin–echo (RARE) localizer sequence [repetition time (TR)=1500 ms, echo time (TE)=19 ms, 5 cm field of view (FOV), 256×256 image matrix giving 195 μm^2 in plane spatial resolution from a 1 mm slice thickness]. The first set of coronal slices was used to establish the position of the knee in the coil. The second set of axial slices through the femoral condyles allowed adjustments to be made to position coronal and sagittal slices. Coronal images to assess OA lesions were easily localized parallel to the posterior femoral condyles [Fig. 1(a)]. To obtain reproducible sections, the sagittal slices were always displayed on the specific axial slice where the arch of the femoral notch described a perfect semi-circumference (‘roman arch view’) and they were perpendicular to a line tangent to the posterior border of the femoral condyles[28]. Nine parasagittal slices (1 mm thickness each) were obtained beginning laterally at the summit of the semi-circumference [Fig. 1(b)]. Two types of sequences were acquired for image analysis: (a) in the sagittal plane, 2D-spoiled gradient-echo with TR/TE=294/13 ms, a flip angle of 60°, 4 NEX and slice thickness 1 mm; and (b) in the coronal plane, 2D-T1 weighted spin–echo with TR/TE=700/24 ms, 2 NEX and 1.5 mm slice thickness. In both cases the FOV was 5 cm and the image acquisition and reconstruction matrix size 256×256. The imaging time for a complete MR examination was 25 min.

MEASUREMENT OF CARTILAGE THICKNESS

The MR images were interpreted by two blinded observers (EC, IP). The sagittal plane was preferred for

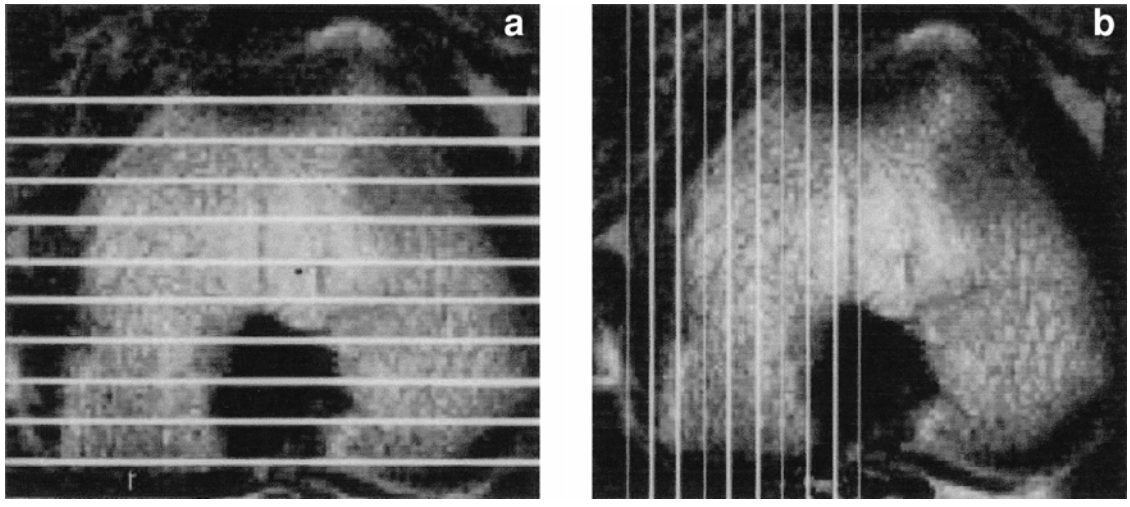

Fig. 1. Fast spin–echo (RARE) axial image through the femoral condyles of the left knee (TR=1500 ms; TE=19 ms). The slices were displayed on the specific axial image where the femoral notch described a perfect semi-circumference ('roman arch view'). (a) Nine coronal slices (1.5 mm thick) were localized parallel to a line tangent to the posterior femoral condyles. (b) Sagittal slices (1 mm thick) perpendicular to a line tangent to the posterior femoral condyles were obtained beginning laterally at the summit of the semi-circumference.

estimations of cartilage thickness because the medial femoral condyle and the medial tibial plateau are more nearly flat in a medial–lateral direction than in a cranial–caudal one. Thus, partial volume errors are minimized by selecting the imaging plane in which the joint tissues vary least through the 1 mm imaging slice. Cartilage thickness was determined in the four central slices of the sagittal images of the medial femoral condyle. The three medial and two lateral parasagittal slices, out of the nine images, were discarded to avoid errors derived from the partial volume effect.

All measurements of cartilage thickness were performed off-line with a home-developed software in UNIX based workstations by using Interactive Data Language (IDL, Research Systems, Boulder, CO). Because in the sagittal plane both the medial femoral condyle and medial tibial plateau resemble a hemisphere, almost all images intersect the cartilage obliquely. This difficulty could be overcome because the software uses a mathematical routine based on analytical geometry that corrects cartilage thickness measurement for oblique distortion. With this program, a hemisphere matched to the condylar and tibial surfaces can be displayed on the image, and lines intersecting perpendicular to the cartilage surface, corresponding to the radius of the hemisphere were used to evaluate cartilage thickness (Fig. 2). After localizing the regions of interest, variations in signal intensity along each perpendicular line (profile) were plotted as a curve with respect to the corresponding distances. Since the cartilage signal intensity is high, it appears as a 'peak' on the profile, while the dips corresponding to the signal drop of the subchondral bone and synovial fluid adjacent to the cartilage are showing the inner and outer edges of the cartilage structures. The hyaline cartilage thickness was estimated computing the distance between these two points on the profile (Fig. 3). A total of 15 femoral and 21 tibial contiguous determinations were performed on each slice. The mean values of cartilage thickness in three equal portions (A=anterior, B=central, C=posterior) of the medial compartment of femur and tibia [Fig. 2(b),(d)] were considered for statistical analysis because thickness of hyaline cartilage can vary at different locations of the joint according to loading characteristics and matrix components[29].

Five distinct morphologic features observable by MRI were in addition selected to study images in both planes: surface irregularities, subchondral bone sclerosis, cysts, osteophytes, and meniscal lesions.

GROSS PATHOLOGY

Immediately after the rabbits were euthanized, the knee joint was dissected. The infrapatellar synovial pad and the femoral and tibial cartilages were inspected by two blinded observers (EC, IP) for gross pathologic changes with the aid of a magnification loupe. The synovial pad was graded as 0 (normal) or 1 (fibrous and proliferative appearance). For the femoral condyle and tibial plateau cartilage the severity of macroscopic changes were categorized as 0 (normal), 1 (discoloration, mild surface irregularities or pitting), 2 (partial thickness erosion or fibrillation), and 3 (full-thickness erosion or osteophytes). An overall score was obtained by adding the severity scores for each lesion recorded.

RADIOGRAPHY

After macroscopic evaluation, anteroposterior and lateral radiographic views of the specimens were taken using a Hewlett-Packard 43805-Faxitron Series tube (25 kV for 20 s, intensity 1.5 mA/s). Each medial femoral condyle was demarcated with a knife and cut into 3 mm sagittal slices with a special sawing device which allowed precise cuts of the bone. A contact X-ray of the sagittal slices was made under the same conditions. The sections were coded and read blindly on an X-ray monitor with a magnification of ×25.

For subchondral bone measurements, the authors used the stereological method of point and intersection counting based on the Cavallieri's principle[30], which allows three-dimensional values of subchondral bone to be obtained

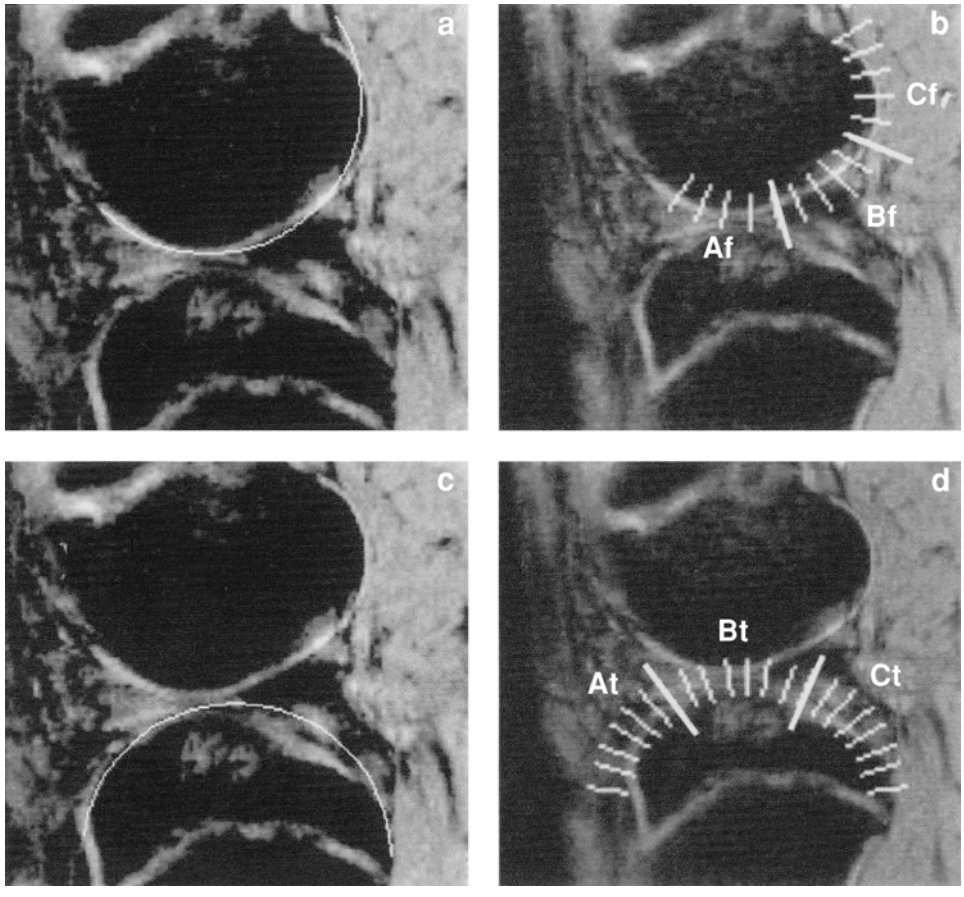

Fig. 2. The cartilage thickness was measured in the sagittal gradient–echo image through the medial compartment of the left knee (TR=294 ms; TE=13 ms). (a) In the femur, a hemisphere matched to the condyle articular surface was displayed on the image. (b) Fifteen perpendicular lines corresponding to the radius of the hemispheres were used to record variations on signal intensity on the articular surface. The mean values of cartilage thickness were calculated in three equal sectors (Af, Bf and Cf) of the hemisphere. (c) A semicircular line tangent to the articular surface was displayed on the tibia. (d) The radius of this line were used to determine the height of tibial cartilage. Three equal portions (Af, Bf and Cf) were also used for statistical analysis.

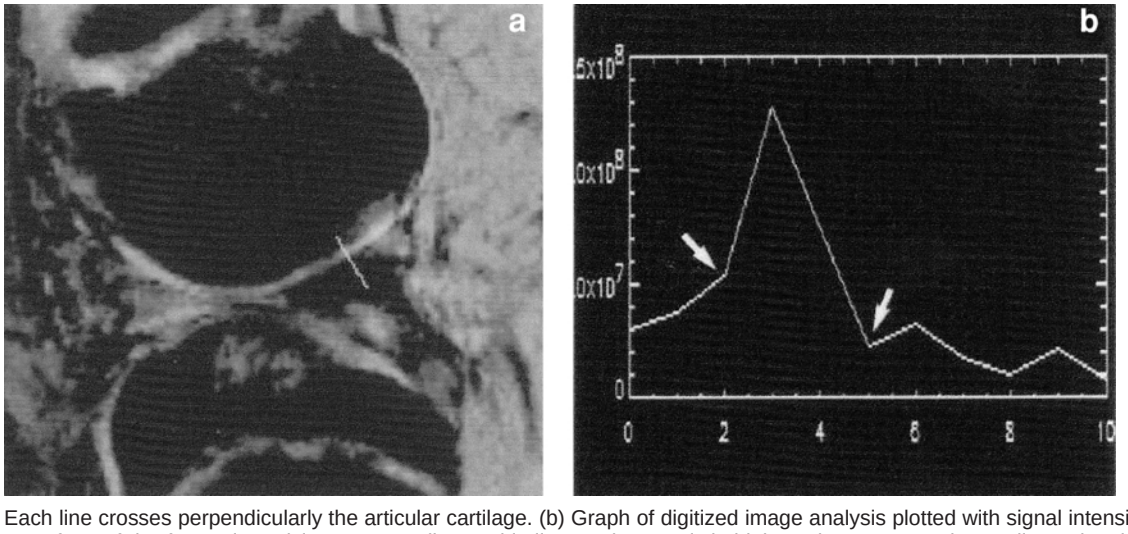

Fig. 3. (a) Each line crosses perpendicularly the articular cartilage. (b) Graph of digitized image analysis plotted with signal intensity across the articular surface of the femoral condyle corresponding to this line. A characteristic high peak represents the cartilage signal intensity. Cartilage thickness was measured computing the distance between the points of signal drop on the baseline corresponding to subchondral bone and joint fluid (arrows).

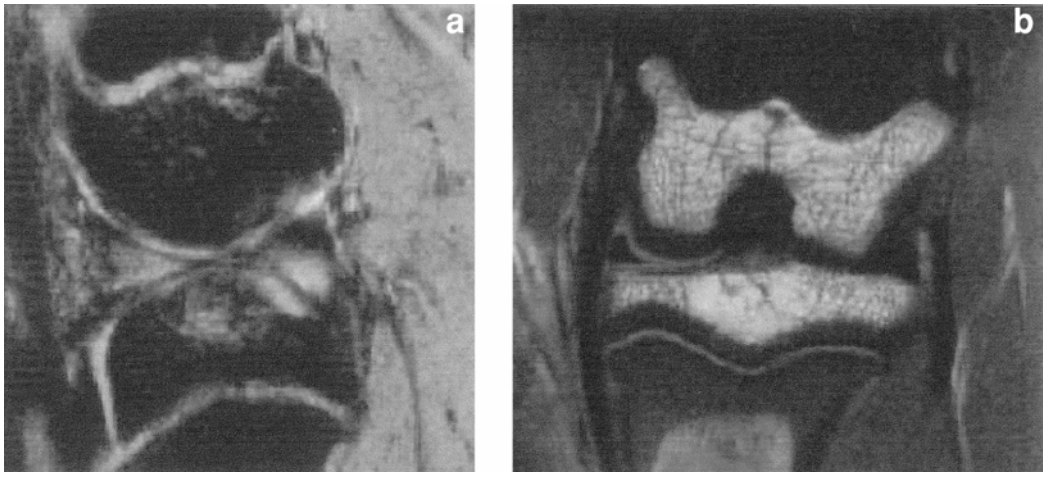

Fig. 4. (a) Sagittal sections through the left knee, extracted from gradient–echo MRI datasets acquired 8 weeks post-operatively. The cartilage shows high signal intensity while the subchondral bone, the menisci and the patellar ligament appear dark. An area of intermediate to high signal intensity can be identified in the trabecular bone under the tibial spines and close to the site of insertion of the posterior cruciate ligament in the femur. The cartilage of the anterior portion of the joint becomes partially blurred after excision of the anterior horn of the meniscus due to the presence of fibrous tissue. (b) Fast spin–echo coronal MRI image of the left knee 8 weeks after partial medial meniscectomy (TR=700 ms; TE=24 ms). The epiphysis displays high signal intensity and the appearance of the subchondral bone is normal. An increase of joint fluid can be observed surrounding the remaining posterior horn of the medial meniscus.

from two-dimensional measurement of the trabecular structure on radiographs. The following estimations were made: (a) trabecular number (number of trabecules vs total volume), (b) bone density (percentage of trabecular bone vs total volume), (c) mean trabecular size (bone trabecular density vs trabecular number), and (d) volume fraction. These data were also analysed separately in the same three portions previously defined for the MRI study. Aside from subchondral bone sclerosis, other radiographic hallmarks of OA, i.e. osteophytes and cysts, were also investigated.

STATISTICAL ANALYSIS

Paired Student *t*-tests were performed on the data to test significant variations on MRI-measured cartilage thickness at previously defined time points. To compare subchondral bone measurements between the groups, the ANOVA and the Mann–Whitney U-tests were used.

Results

MRI ASSESSMENT OF MACROSCOPIC CHANGES

In spin–echo coronal sections the cartilage high signal intensity disappeared and bone tissue, menisci and ligaments remained dark, but fat showed intermediate to high signal intensity [Fig. 4(a)]. A well-defined layer of subchondral bone was visible and the epiphyseal trabecular bone demonstrated its classic uniform alveolar structure. While fat shows high signal intensity related to bone in this sequence, it seems to be well suited to study changes in subchondral bone. However, bony changes involving the development of cysts, osteophytes and sclerosis could not be identified. The site of the anterior horn of the removed medial meniscus was occupied by fibrous tissue and hemosiderin deposits in the slices intersecting the anterior part of the joint. An increment in joint fluid in the medial compartment of the knee was also observed.

Whereas hyaline cartilage showed high signal intensity in gradient–echo images, cortical and subchondral bone, the remaining menisci, the patellar and cruciate ligaments and the subcutaneous and fatty zones appeared dark [Fig. 4(b)]. The articular cartilage preserved a homogeneous appearance without identifiable surface irregularities all over the study. In sagittal sections close to the femoral intercondylar notch, MRI showed areas of high signal intensity in the subchondral bone located under the tibial spines and in the vicinity of the origin of the posterior cruciate ligament in the posterior part of the femoral condyle. This image was observed in both operated and non-operated animals, and was therefore considered not related to the osteoarthritic process. MRI changes corresponding to edema and hemosiderin deposits secondary to surgery were obvious post-operatively in the synovium and the surrounding tissues in both meniscectomized and sham-operated animals.

MEASUREMENT OF CARTILAGE THICKNESS (TABLE I)

MR images of the normal rabbit knee showed cartilage as an isolated band of high signal intensity located between adjacent intermediate to low signal intensity of joint fluid and subchondral bone. In the anterior part of the joint, the image of the cartilage became frequently blurred in operated rabbits due to post-operative edema and fibrosis, and the peak corresponding to cartilage tissue in the computerized profile could not be readily identifiable.

Although overall articular cartilage of both femur and tibia showed a trend to increase in thickness over the time, the differences were not statistically significant at any of the five time points when compared with pre-operative values. However, cartilage thickness at the weight-bearing area of the femur (sector Bf) demonstrated a significant increase by 4 weeks, and this increment was progressive up to 8 weeks post-operatively ($P<0.05$). On the other hand, a significant increment in tibial cartilage thickness could only be detected at week 6, and it was also located at the central

Table I
Cartilage thickness (mean±standard deviation in mm)

Region*	Week 0	Week 2	Week 4	Week 6	Week 8	Week 10
Af	0.64±0.16	0.59±0.19	0.63±0.18	0.64±0.18	0.57±0.14	0.65±0.19
Bf	0.58±0.14	0.59±0.13	0.62±0.16†	0.67±0.16†	0.72±0.19†	0.58±0.16
Cf	0.56±0.12	0.56±0.12	0.59±0.14	0.62±0.13	0.63±0.09	0.67±0.19
At	0.69±0.73	0.57±0.15	0.63±0.13	0.72±0.18	0.63±0.21	0.59±0.18
Bt	0.62±0.16	0.62±0.16	0.64±0.21	0.68±0.21‡	0.62±0.15	0.59±0.18
Ct	0.64±0.17	0.58±0.18	0.59±0.14	0.66±0.24	0.59±0.17	0.68±0.11

*Af, anterior region of the medial femoral condyle; Bf, central region of the medial femoral condyle; Cf, posterior region of the medial femoral condyle; At, anterior region of the medial tibial plateau; Bf, central region of the medial tibial plateau; Cf, posterior region of the medial tibial plateau.
† and ‡ represent statistically significant values vs time 0 in the femur and tibia respectively ($P<0.05$).

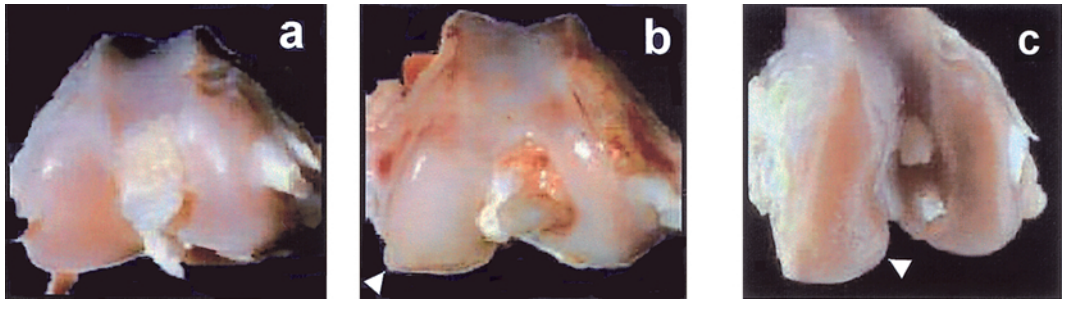

Fig. 5. Gross pathological macrographs of the left femoral condyle (a) Femoral articular surface of the left knee from a normal control rabbit. (b) Six weeks after partial medial meniscectomy the normal whitish bright appearance of the femoral cartilage disappears, especially in the load bearing region. Note the irregularity at the medial rim of the posterior condyle corresponding to an initial osteophyte (arrowhead). (c) In this sample obtained 10 weeks after the operation the discoloration is more evident, especially in the posterior femoral condyle, where ulcers, fissuring and pitting can also be observed (arrowhead).

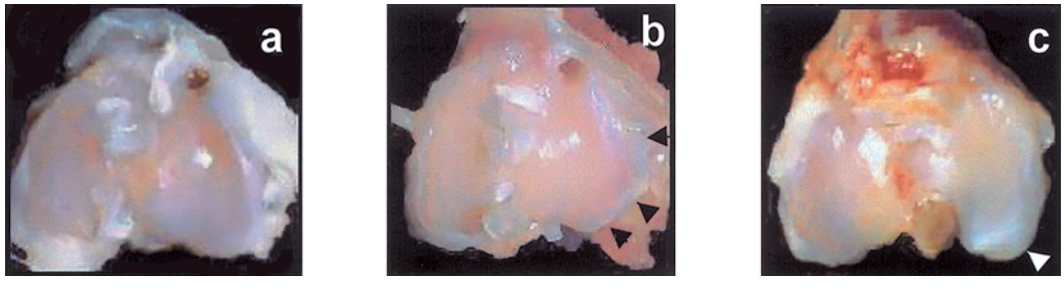

Fig. 6. Gross pathological macrographs of the left tibial plateau at various stages of OA. (a) Normal articular surface showing the whitish smooth cartilage. (b) Six weeks post-meniscectomy the cartilage clearly shows an inflamed irregularity of the medial tibial cartilage contour corresponding to an ostephyte (arrowheads). (c) Changes of OA, including eburnation of the articular surface and an osteophyte at the edge of the medial tibial plateau, are seen in this specimen assessed 10 weeks after the operation (arrowhead).

region of the medial tibial plateau (sector Bt) ($P<0.05$). The two rabbits imaged 10 weeks after surgery also had a higher increment in cartilage height, but the difference was not significant, probably due to insufficient data.

GROSS PATHOLOGY

No abnormalities could be found on gross inspection in the normal rabbits and the sham-operated controls showed only mild sinovial thickening located at the medial parapatellar fat pad, where the joint had been opened [Figs 5(a) and 6(a)]. In the partial meniscectomy series, fibrous tissue proliferation could be observed at the site where the meniscus had been removed, extending to the patellar fat pad and the anterior medial compartment of the knee. This tissue overlaid, but was not adherent to, the articular surface. At the earliest stages of the isease (2 and 4 weeks post-operatively) two rabbits showed mild abnormalities, i.e. cartilage discoloration or mild synovial thickening. Synovium was grossly abnormal in most knees from 6 weeks after partial meniscectomy, with obvious thickening and a pale yellow-orange appearance. At 6 weeks the articular cartilage of two osteoarthritic animals had clearly lost its brightness. Two rabbits also revealed some areas of pitting and presented a small initial osteophyte at the medial rim of both, the femoral condyle and tibial plateau [Fig. 5(b) and 6(b)]. These abnormalities were also evident at 8 weeks. The changes in coloration were more marked in those rabbits examined 10 weeks post-meniscectomy, especially in the weight-bearing areas of the medial compartment of

Table II
Cancellous bone structure morphometry for osteoarthritic and control groups (mean±standard deviation)

	6 weeks	10 weeks
Trabecular number (no./mm^3)		
Control	34±7	28±1
Sham	30±8	32.3±7
Osteoarthritic	27±4	29.3±3
Bone density (%)		
Control	53±10	55±1
Sham	52±4	44±10
Osteoarthritic	54±3	56±4
Trabecular size (mm)		
Control	0.02±0.001	0.02±0.001
Sham	0.02±0.01	0.01±0.001
Osteoarthritic	0.02±0.003	0.02±0.02
Volume fraction (%)		
Control	84±1	82.5±0.5
Sham	84±1	81.2±1
Osteoarthritic	78.6±6	81.2±1

the knee, where the articular surface appeared markedly eburnated [Fig. 5(c) and 6(c)]. Erosions and osteophytes could in addition be observed in four of the five samples assessed. Ulcers were very small in diameter (0.5 mm), partial-thickness, and predominantly localized at the medial and posterior aspects of the femoral condyle. Here osteophytes were small and developed at the margin of the posterior femoral condyle [Fig. 5(c)]. On the other hand, the edge of the medial tibial plateau exhibited a more extensive thickening and remodeling, with osteophytes measuring up to 1 mm. In the posteromedial rim, the osteophytes appeared as a thin white colored margin bordering the medial compartment [Fig. 6(c)]. This appearance led us to believe that they were mainly of cartilaginous instead of osseous nature, representing early soft spurs (chondrophytes). No osteophytes or other cartilaginous defects were found in the lateral compartment of the meniscectomized knees.

HISTOQUANTITATION OF SUBCHONDRAL BONE

Anteroposterior and lateral X-rays of the whole joint taken at 6 and 10 weeks were normal. The differences between bone structure parameters of the bone blocks did not reach statistical significance between osteoarthritic and control rabbits at either of the two time points considered (Table II). Neither did the comparison of 6 vs 10 week data in the operated group reveal statistical significance. For each of the histomorphometric variables analyzed, the variance of the osteoarthritic group is markedly increased compared with the control groups.

Discussion

Numerous MRI sequences have been proposed to enhance contrast between hyaline cartilage and adjacent structures[7,9,33]. Gradient–echo sequences offer a wide choice of contrasts and allow volume (three-dimensional) data**.** Among these, sequences with short TEs and relatively large flip angles provide T1-weighted images where the intraarticular fluid is less intense than the cartilage and fat is effectively suppressed maximizing the contrast between cartilage, fluid and marrow[17]. Thus, fat-suppressed sequences have been shown to offer an excellent compromise for estimating quantitatively articular cartilage[4]. The optimized fat-suppressed gradient–echo sequence used in our study provided high contrast between cartilage and surrounding structures. This was confirmed when variations in signal intensity were automatically registered as a profile, where a clearly defined peak showed the increase in intensity corresponding to cartilage.

In addition to contrast problems, cartilage has also proven difficult to evaluate accurately with MRI due to the limits of spatial resolution, since it represents a thin layer of material relative to the size of the voxels that are typically used for MRI. We addressed this difficulty by using high field strength gradients. This system allows a high signal-to-noise ratio per unit time, which offers the advantages of both thinner sections and smaller fields of view. Investigations of cartilage using high field strength have recently shown that qualitative information derived from high resolution MRI correlates extremely well with histologic findings; nevertheless, this technology had not yet been applied to quantitative studies[9,10,32]. One of the limitations of cartilage measurements is the poor correlation between determinations made on MRI with those performed on anatomic sections[33]. This problem can be partly overcome with the higher spatial resolution obtained in our study, and for some applications consistent under or overestimation of the cartilage thickness would not be a serious problem because it would still allow longitudinal changes in the same joint to be quantified. It could be argued that transferring this protocol and results to a clinical environment could be difficult because the differences between the experimental and control animals were small and because this model employed a high-field, small-bore magnet, which provides high resolution but might not be applicable to humans. However, this study was performed over short periods of time at the very early stages of the disease, and in clinical practice it is not necessary to assess cartilage thickness variations at time points so close to each other. In addition, human articular cartilage is much bigger than that of the rabbit; therefore it seems reasonable to think that variations in early OA in humans would be more marked and an MRI system with such a high resolution is probably not necessary.

MRI can very accurately depict morphologic changes in OA. These could not be detected in this study, either in cartilage or in subchondral bone, because the joint was imaged in the earlier stages of the disease when those alterations are still not detectable. Other early abnormalities accessible to MRI include signal modification of the cartilage, as well as focal thinning and thickening. These changes may be visible as either focal variations in signal intensity in the cartilage[18,34] or as an alteration of its plurilaminar appearance[10,18,19]. However, the appearance of the layers varies greatly according to the pulse sequences, and recent studies have demonstrated that truncation artefacts can produce false laminae[35,36].

Because morphologic alterations might not be detected in the earlier stages of the disease and could be due to artefacts, a quantitative approach is necessary to study the early MRI changes in the evolution of OA. In addition to estimation of changes in T1 and T2 relaxation times, a quantitative assessment of cartilage alterations can be obtained with determinations of cartilage thickness[25,26,31,37]. Other investigators have used volumetric studies to obtain more accurate cartilage analysis with promising preliminary results[8,23], but these MR techniques

increase the examination time and require an additional reconstruction period, augmenting the global evaluation time substantially. For the measurement of cartilage thickness we used an MRI protocol that allowed us to outline the cartilage, but a sequential evaluation also requires precise realignment of the section location and orientation, otherwise changes of cartilage thickness cannot be reliably quantified from serial images. Slight misalignment or poor stabilization of the knees would produce errors when obtaining sagittal images. Furthermore, partial volume effect can alter the appearance of thin cartilage structures as a function of the orientation of the imaging plane relative to the cartilage. Since these errors are additive, they might give rise to large inaccuracies. Although no test–retest assessment of cartilage thickness measurement demonstrating that the determinations were repeatedly done at the same locations was performed in this study, the method of knee orientation adopted allowed a clear recognition of the precise topography of each portion of cartilage and permitted reproducible imaging planes to be obtained. A precise analytic technique for generating curves matching the femoral and tibial surfaces, where the measurement of cartilage thickness could be repeated, was also developed.

As the cartilage–joint fluid interface is difficult to define by MRI, while the bone cartilage interface is usually clear, numerous experiments measure the thickness of cartilage using the distance between the opposite bony margins[26,37]. The computerized technique used here is capable of detecting minimal changes in signal intensity and the cartilage plate can be easily distinguished from adjacent structures; we were therefore able to study femur and tibia separately and to assess the variations in different zones. The use of high field strength combined with a method of automated measurement of cartilage thickness based on the application of digitized image analysis furnishes an alternative technique which has been demonstrated to be more accurate than those derived from naked eye assessment[24] employed by other authors[16,25,26,37], which depends on subjective value judgements such as how to define the boundaries of cartilage and are extremely tedious for quantitative longitudinal studies where large numbers of samples are to be studied sequentially. The technique described in this work is also especially valuable in estimation of small, tight joints containing minimal or no joint fluid between the two opposing cartilage surfaces.

Many MRI investigations of osteoarthritic joints have described either thickening or thinning of hyaline cartilage[15,37–39]. In experimental MRI sequential determinations of its thickness, an initial phase of cartilage hypertrophy followed by degeneration and loss has been identified[26,34]. This initial phase of hypertrophic remodeling, preceding cartilage erosion and loss has ben related to ultrastuctural alterations such as an increase in water content[40,41]. Animal studies have even suggested that cartilage thickness may dynamically adapt to immobilization and exercise by atrophy and hypertrophy respectively[8]. Then, quantitative estimations in early OA might depend on the specific grade of activity and stage of the disease when the measurements were performed, and the different results published in the literature could simply reflect this relationship during OA progression. In the present work we chose to study the changes in the rabbit knee as previous investigations had demonstrated by histology the occurrence of cartilage lesions very similar to those seen in early human knee OA[27]. In addition, cartilage thickness at the medial compartment of the knee remains unchanged during maturation in healthy rabbits[42]. Thus, errors derived from a theoretical increment in thickness of cartilage due to animal growth were excluded. Furthermore, this model induces a mild focal form of the disease that, although progressive, results in relatively little joint destruction up to several months after surgery, which makes it suitable for longitudinal MRI studies of early changes[43]. Subsequently, the increasing focal height found in femoral cartilage after surgery can be considered as the earliest change measurable with MRI in OA. It seems likely that cartilage loss and degeneration would be appreciated in similar study performed in joints with moderate and severe OA. Cartilage surface abnormalities such as osteophytes demonstrated on gross inspection of the knee, could probably not be detected in our MR images because they were localized at the periphery of the femoral and tibial cartilage, and the medial and lateral parasagittal slices were discarded in this study.

The finding of an increase in cartilage height at the central sector of the medial femoral condyle is consistent with the observations of Moskowitz *et al*., who described the earliest abnormalities in cartilage to be localized primarily at the same part, normally in contact with the tibial plateau[27]. The cartilage of the rabbit knee joint is both thicker and stiffer at the central and posterior areas of the femoral condyle than the anterior area[29]. These regional variations are related to the specific anatomical construction and behavior of the animal, suggesting that the posterior femoral condyle might be loaded more than the anterior one because, under normal conditions, the rabbit stands and walks with the knee flexed. Other animal studies have also shown a correlation between articular cartilage thickness and the compressive stress borne by the joint surface, and a higher thickness of cartilage indicating abnormal functional requirements of the articular surface[42,44].

Little attention has been paid to the MRI diagnosis of subchondral bone changes in OA, even though there are suggestions that primary OA could initially be a bone disease rather than a cartilage disease. The majority of MRI investigations on bone-remodeling changes in OA have also been focused on the detection of morphologic alterations, which appear in advanced stages[19,20,22]. An MRI-controlled method for quantitatively monitoring the progression of bone damage in OA has recently been described[21], but the parameters studied were not compared to controls, and were assessed at an interval of time that corresponds to a moderate and advanced stage of the disease. When studying subchondral bone, a ‘normal control’ population is mandatory in order to separate categorically the effects of normal maturation of the subchondral plate from pathologic sclerosis. Since MRI did not detect changes in our study, we also assessed subchondral bone with microfocal radiography. On the radiographs we could not find differences in the structure parameters. The data obtained in this work strongly suggest that in this model cartilage lesions precede major structural changes (sclerosis) of the subchondral bone. Further studies are needed to evaluate the MRI appearance of degenerative changes in subchondral bone later in the course of the disease in this experimental model.

In summary, MRI has been demonstrated to be a useful method for the assessment of very early joint damage in the evolution of the disease, particularly relevant since it is non-invasive and allows longitudinal follow-up. The use of MR high field strength in combination with a method of

computerized measurement of cartilage thickness appears promising in quantitative assessment of articular cartilage. This study demonstrates that an increase in cartilage thickness in the areas bearing weight is one of the earliest measurable changes in OA. Those alterations in cartilage thickness observed by MRI preceded structural alterations in subchondral bone. To evaluate the potential beneficial effect of novel therapies with disease-modifying activities it is essential to quantitatively monitor the early changes in OA, and MRI is a useful technique that can be used for this purpose.

References

1. Altman RD, Fries JF, Bloch DA, Carstens J, Cooke TD, Genant H, *et al*. Radiographic assessment of progression in osteoarthritis. Arthritis Rheum 1987;30:1214–25.
2. Howell DS, Treadwell BV, Trippel SB. Etiopathogenesis of osteoarthritis. In: Moskowitz RW, Howell DS, Goldberg VM, Mankin HJ, Eds. Osteoarthritis. Diagnosis and Medical/Surgical Management. London: Saunders 1992:233–54.
3. Hodler J, Resnick D. Current status of imaging of articular cartilage. Skeletal Radiol 1996;25:703–9.
4. Leouille D, Olivier P, Mainard D, Gillet P, Netter P, Blum A. Magnetic resonance imaging of normal and osteoarthritic cartilage. Arthritis Rheum 1998;41:963–75.
5. Peterfy CG, Genant HK. Emerging applications of magnetic resonance imaging in the evaluation of articular cartilage. Radiol Clin North Am 1996; 34:195–213.
6. Hutton CW, Vennart W. Osteoarthritis and magnetic resonance imaging: potential and problems. Ann Rheum Dis 1995;54:237–43.
7. Bacic G, Liu KJ, Goda F, Hoopes PJ, Rosen GM, Swartz HM. MRI contrast enhanced study of cartilage proteoglycan degradation in the rabbit knee. Magn Reson Med 1997;37:764–8.
8. Eckstein F, Schnier M, Haubner M, Priebsch J, Glaser C, Englmeier KH, *et al*. Accuracy of cartilage volume and thickness measurements with magnetic resonance imaging. Clin Orthop 1998;352:137–48.
9. Dawson J, Gustard S, Beckmann N. High-resolution three-dimensional magnetic resonance imaging for the investigation of knee joint damage during the time course of antigen-induced arthritis in rabbits. Arthritis Rheum 1999;42:119–28.
10. Leouille D, Gonord P, Guingamp C, Gillet P, Blum P, Blum L, *et al*. In vitro magnetic resonance microimaging of experimental osteoarthritis in the rat knee joint. J Rheumatol 1996;24:133–9.
11. Blackburn WD, Bernreuter WK, Rominger M, Loose LL. Arthroscopic evaluation of knee articular cartilage: A comparison with plain radiographs and magnetic resonance imaging. J Rheumatol 1993;21:675–9.
12. McAlindon TEM, Watt I, McCrae F, Goddard P, Dieppe PA. Magnetic resonance imaging in osteoarthritis of the knee: correlation with radiographic and scintigraphic findings. Ann Rheum Dis 1991;50:14–9.
13. Munasinghe JP, Tyler JA, Hodgson RJ, Barry MA, Gresham GA, Evans R, *et al*. Magnetic resonance imaging, histology, and X-ray of three stages of damage to the knees of STR/OTR mice. Invest Radiol 1996;10:630–8.
14. Chan WP, Lang P, Stevens MP, Sack K, Majumdar S, Stoller DW, *et al*. Osteoarthritis of the knee: Comparison of radiography, CT, and MR imaging to assess extent and severity. AJR 1991;157:799–806.
15. Adams ME, Li DKB, McConkey JP, Davidson RG, Day B, Duncan CP, *et al*. Evaluation of cartilage lesions by magnetic resonance imaging at 0.15T: Comparison with anatomy and concordance with arthroscopy. J Rheumatol 1991;18:1573–80.
16. Modl JM, Sether LA, Haughton VM, Kneeland JB. Articular cartilage: Correlation of histologic zones with signal intensity at MR imaging. Radiology 1991;181:853–5.
17. Recht MP, Kramer J, Marcelis S, Pathria MN, Trudell D, Haghighi P, *et al*. Radiology 1993;187:473–8.
18. Gahunia HK, Babyn P, Lemaire C, Kessler MJ, Pritzker KPH. Osteoarthritis staging: comparison between magnetic resonance imaging, gross pathology and histopathology in the rhesus macaque. Osteoarthritis Cart 1995;3:169–80.
19. Carpenter TA, Everett JR, Hall LD, Harper GP, Hodgson RJ, James MF. Visualization of subchondral erosion in rat monoarticular arthritis by magnetic resonance imaging. Skeletal Radiol 1995;24:341–9.
20. Nolte-Ernstring CCA, Adam G, Bühne M, Prescher A, Günther RW. MRI of degenerative bone marrow lesions in experimental osteoarthritis of canine knee joints. Skeletal Radiol 1996;25:413–20.
21. Watson PJ, Hall LD, Malcolm A, Tyler JA. Degenerative joint disease in the guinea pig. Arthritis Rheum 1996;8:1327–37.
22. McGibbon CA, Dupuy DE, Palmer WE, Krebs DE. Cartilage and subchondral bone distribution with MR imaging. Acad Radiol 1998;5:20–5.
23. Peterfy CG, van Dijke CF, Lu Y, Nguyen A, Connick TJ, Kneeland JB, *et al*. Quantification of the volume of articular cartilage in the metacarpophalangeal joints of the hand: Accuracy and precision of three-dimensional MR imaging. AJR 1995;165:371–5.
24. Tan TCF, Wilcox DM, Frank L, Shih C, Trudell D, Sartoris DJ, *et al*. MR imaging of articular cartilage in the ankle: comparison of available imaging sequences and methods of measurement in cadavers. Skeletal Radiol 1996;25:749–55.
25. Klandy B, Bail H, Swoboda B, Schiwi-Bochat H, Beyer WF, Weseloh G. Cartilage thickness measurement in magnetic resonance imaging. Osteoarthritis Cart 1996;4:181–6.
26. Watson PJ, Carpenter TA, Hall LD, Tyler JA. Cartilage swelling and loss on a spontaneous model of osteoarthritis visualized by magnetic resonance imaging. Osteoarthritis Cart 1996;4:197–207.
27. Moskowitz RW, Davis W, Sammarco J, Martens M, Baker J, Mayor M, *et al*. Experimentally induced degenerative joint lesions following partial meniscectomy in the rabbit. Arthritis Rheum 1973;16:397–405.
28. Goutallier D, Bernageau J, Lecudonnec B. Mesure de l'écart tubérosité tibiale antérieure–gorge de la trochlée: TA-GT. Rev Chir Orthop 1978;64:423–8.
29. Räsänen T, Messner K. Regional variations and indentation stiffness and thickness of normal rabbit knee articular cartilage. J Biomed Mat Res 1996;31:519–24.
30. Gundersen HJ, Bendtsen TF, Korbo L, Marcussen N, Moller A, Nielsen K, *et al*. Some new, simple and

efficient stereological methods and their use in pathological research and diagnosis. APMIS 1988;96:379–94.
31. Robson MD, Hodgson RJ, Herrod NJ, Tyler JA, Hall LD. A combined analysis and magnetic resonance imaging technique for computerised automatic measurement of cartilage thickness in the distal interphalangeal joint. Magn Reson Imaging 1995;13:709–18.
32. Xia Y, Farquhar T, Burton-Wurster N, Ray E, Jelinsky LW. Diffusion and relaxation mapping of cartilage–bone plugs and excised disks using using microscopic magnetic resonance imaging. Magn Reson Med 1994;31:273–82.
33. Hodler J, Loredo RA, Longo C, Trudell D, Yu JS, Resnick D. Assessment of articular cartilage thickness of the humeral head: MR-anatomic correlation in cadavers. AJR 1995;165:615–20.
34. Gahunia HK, Lemaire C, Babyn PS, Cross AR, Kessler MJ, Pritzker KPH. Osteoarthritis in rhesus macaque knee joint: Quantitative magnetic resonance imaging tissue characterization of articular cartilage. J Rheumatol 1995;22:1747–56.
35. Erickson SJ, Waldschmidt JG, Czervionke LF, Prost RW. Hyaline cartilage: Truncation artifacts as a cause of trilaminar appearance with fat-suppressed three-dimensional spoiled gradient-recalled sequences. Radiology 1996;201:260–4.
36. Frank LR, Brossmann J, Buxton RB, Resnick D. MR imaging truncation artifacts can create a false laminar appearance in cartilage. AJR 1997;168:547–54.
37. Paul PKP, O'Byrne E, Blancuzzi V, Wilson D, Gunson D, Douglas FL, *et al*. Magnetic resonance imaging reflects cartilage proteoglycan degradation in the rabbit knee. Skeletal Radiol 1991;20:31–6.
38. Braunstein EM, Brandt KD, Albrecht M. MRI demonstration of hypertrophic articular cartilage repair in osteoarthritis. Skeletal Radiol 1990;19:335–9.
39. Herberhold C, Stammberger T, Faber S, Putz R, Englmeier KH, Reiser M, *et al*. An MR-based technique for quantifying the deformation of articular cartilage during mechanical loading in an intact cadaver joint. Magn Reson Med 1998;39:843–50.
40. McDevitt CA, Muir H, Gilbertson E. An experimental model of osteoarthritis. Early morphological and biochemical changes. J Bone Joint Surg 1977;59B:24–35.
41. Adams ME. Cartilage hypertrophy following canine anterior cruciate ligament transection differs among different areas of the joint. J Rheumatol 1988;16: 818–24.
42. Wei X, Räsänen T, Messner K. Maturation-related compressive properties of rabbit knee articular cartilage and volume fraction of subchondral tissue. Osteoarthritis Cart 1998;6:400–9.
43. Shapiro F, Glimcher MJ. Induction of osteoarthrosis in the rabbit knee joint: Histologic changes following meniscectomy and meniscal lesions. Clin Orthop 1980;147:287–95.
44. Akizuki S, Mow VC, Muller F, Pita JC, Howell DS. Tensile properties of human knee joint cartilage: II. Correlations between weight bearing and tissue pathology and the kinetics of swelling. J Orthop Res 1987;5:173–86.